European Polymer Journal 196 (2023) 112290

Contents lists available at ScienceDirect

European Polymer Journal

journal homepage: www.elsevier.com/locate/europolj

Recyclable dual-curing thiol-isocyanate-epoxy vitrimers with sequential relaxation profiles

Sasan Moradi *, Xavier Fernández-Francos, Osman Konuray *, Xavier Ramis

Thermodynamics Laboratory, ETSEIB Universitat Politècnica de Catalunya, Av. Diagonal 647, 08028 Barcelona, Spain

ARTICLE INFO

Keywords:
Vitrimers
Poly(thiourethane)
Isocyanate
Dual-curing
Thermosets
Recycling
Epoxy
Thiol

ABSTRACT

Two series of poly(thiourethane)s-poly(thiol-epoxy) hybrids were prepared from dual-curing, stoichiometric thiol:isocyanate:epoxy mixtures. 1-methylimidazole (MI) was used as initiator for the thiol-isocyanate and thiol-epoxy curing reactions. A salt of tetraphenylborate derived from highly basic amine 1,5,7 triazabicyclo [4,4,0] dec-5-ene (TBD) was used as catalyst for the activation of bond exchange reactions. The curing kinetics and the glass transition temperature (Tg) of the samples were studied by differential scanning calorimetry (DSC). Thermal stability was characterized by thermogravimetric analysis (TGA). Stress relaxation dynamics related to the bond exchange reactions were studied by dynamic mechanical analysis (DMA). Recyclability of the fully cured samples according to the DMA results was carried out by hot-pressing at elevated temperatures. The results show that the curing process takes place in a controlled and sequential way: the thiol-isocyanate reaction takes place first, at moderate temperatures, followed by the thiol-epoxy reaction, which is completed at higher temperatures. The analysis of stress relaxation evidences a complex two-step relaxation behavior depending on the contribution of isocyanate and epoxy groups to the mixture. Isocyanate-rich materials show a simple relaxation process corresponding to the *trans*-thiocarbamoylation exchange reactions. Epoxy-rich materials show, in contrast, a two-step relaxation processes evidencing that *trans*-thiocarbamoylation alone may not be sufficient to relax the stress completely, due to an apparently permanent network structure. However, complete stress relaxation is possible for epoxy-rich materials through additional bond exchange reactions such as transesterification or dynamic thiol-Michael, but at a slower rate. Depending on the composition and the temperature, full recycling of the material can be achieved at moderate temperatures in a timescale of minutes to hours.

1. Introduction

In general, polymers are classified into two categories based on their thermal response: thermoplastics and thermosets. Among thermoplastics, amorphous thermoplastics soften at temperatures above their T_g, which allows them to be processed and recycled. This property makes thermoplastics attractive for a wide range of basic products and consumer goods. However, their poor mechanical properties and lack of chemical resistance render them inadequate for certain advanced applications. In contrast, thermosetting polymers have superior mechanical and thermal properties thanks to their highly cross-linked structure that allows them to be widely used in demanding applications [1,2]. Perhaps epoxy resins are the most well-known thermosets, which are ubiquitous due to their good adhesion properties, light weight, durability and versatility. These traits still incite researchers around the world to develop new epoxy –based polymers.

Despite their numerous advantages, a main drawback of thermosets is that they cannot be recycled or reprocessed after being fully cured due to their crosslinked network structure, which can have a serious environmental impact [3]. The development of covalent adaptable networks (CANs) [4] and vitrimers [5] in recent years made it possible to design materials combining the advantages of thermosets and thermoplastics. During the last decade, covalent adaptable networks (CANs) have received much attention, leading to the discovery and the incorporation of a wide range of dynamic bond exchange reactions into thermosets [6,7]. Some of the most popular bond exchange reactions used in thermosets include transesterification [8–10], *trans*-thiocarbamoylation [11–13], disulfide exchange [14–17] and imine exchange [18–21]. The preparation of materials combining different bond exchange mechanisms with clearly different kinetics was recently reported [15]. The possibility of achieving complete stress relaxation with a controlled fraction of permanent (non-dynamic) bonds was also recently

* Corresponding authors.
E-mail addresses: sasan.moradi@upc.edu (S. Moradi), ali.osman.konuray@upc.edu (O. Konuray).

https://doi.org/10.1016/j.eurpolymj.2023.112290
Received 5 May 2023; Received in revised form 28 June 2023; Accepted 10 July 2023
Available online 13 July 2023

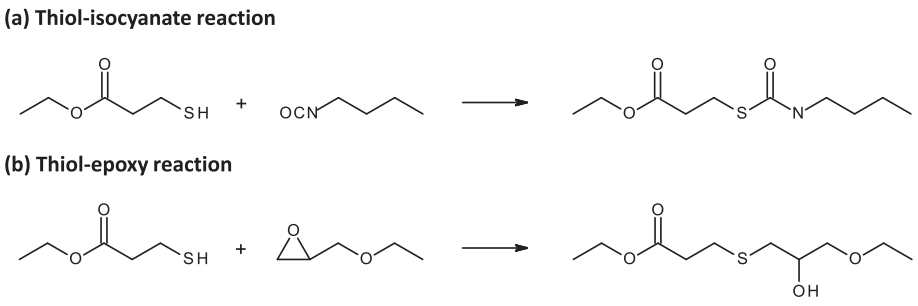

Scheme 1. (a) Thiol-isocyanate and (b) thiol-epoxy reactions

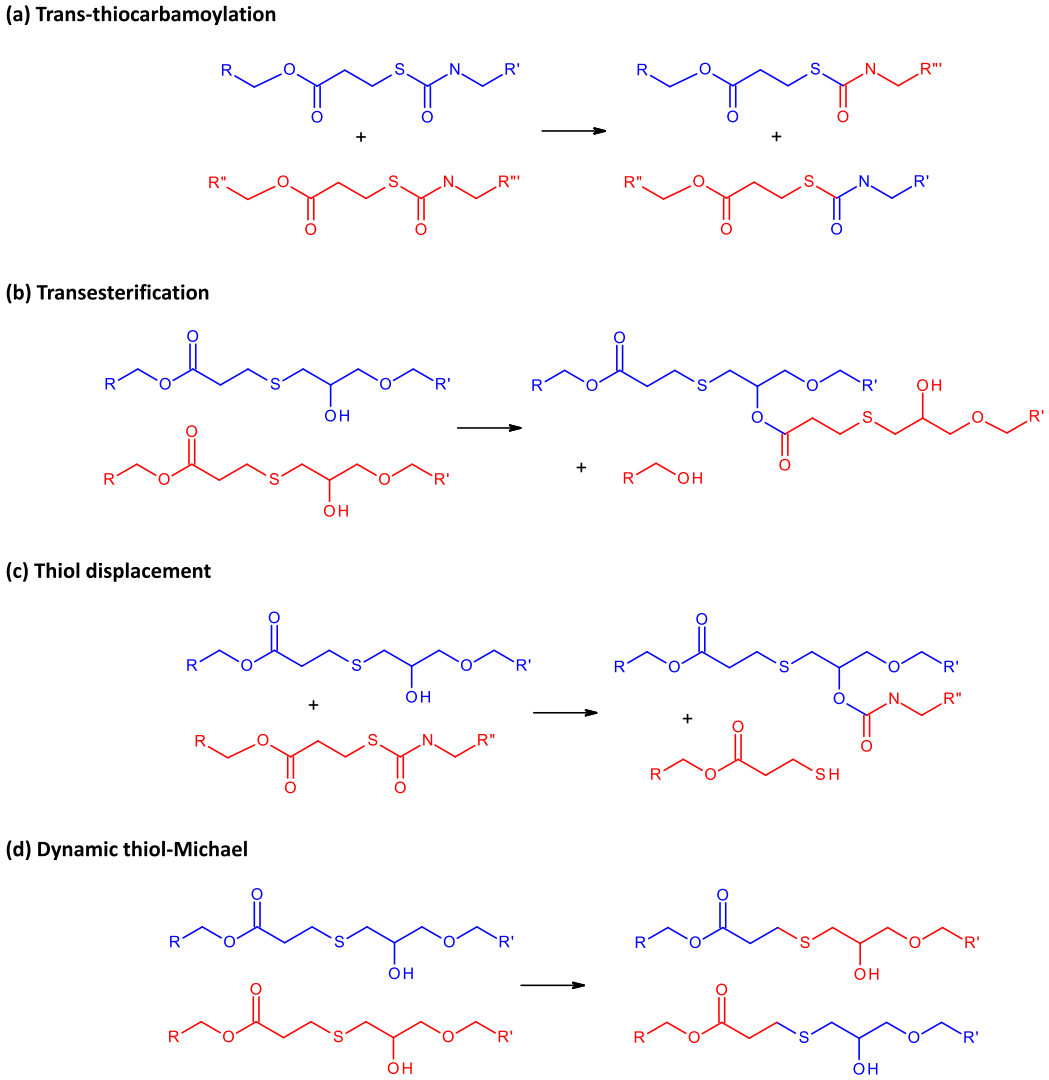

Scheme 2. Bond exchange reactions taking place in the polymer networks analyzed in this work.

demonstrated [10,15]. In this context, an excessive fraction of permanent bonds would lead to controlled and incomplete stress relaxation. As a matter of fact, such features can be predicted and modeled from a statistical perspective [10,15,22].

In this work we explore a new concept of CAN based on the combination of two bond exchange reactions with highly disparate kinetics, prepared following a dual-curing processing scheme. We combine the processing flexibility and structural design capabilities of dual-curing systems [23–26] with the additional reprocessing and recycling capabilities of CANs. To that end, we choose to prepare dual-curing thermosets based on stoichiometric ternary thiol-isocyanate-epoxy mixtures in which the thiol-isocyanate reaction takes place first, followed by the thiol-epoxy reaction [27], as seen in Scheme 1.

Such sequential dual-curing behavior has also been observed for ternary thiol-isocyanate-acrylate systems [28] and thiol-acrylate-epoxy systems [29,30]. All these systems are based on base- or nucleophile-catalyzed thiol-click additions, in which the sequential character is guaranteed by the selective addition of the active thiolate species to the different acceptors. In some cases, such selective addition needs to be controlled by choosing suitable temperatures [29]. In the present case,

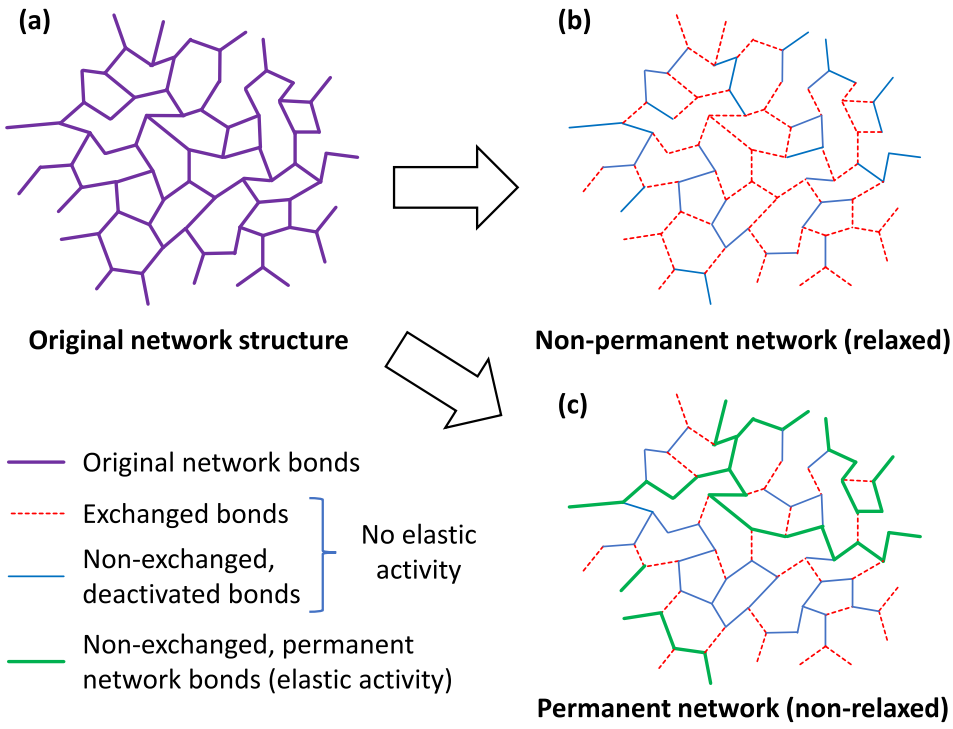

Fig. 1. Effect of the removal of the dynamic bonds from the (a) original network structure, leading to (b) a non-permanent, relaxed structure with no elastic activity or else (c) a permanent non-relaxed network structure with elastic activity.

addition of the thiolate anion to the isocyanate is much faster than that to the epoxy, which can take place once the isocyanate groups have been exhausted. These polymer networks contain a number of dynamic bonds that can be exchanged following different mechanisms, represented in Scheme 2.

Primarily, the thiourethane bonds produced by the thiol-isocyanate reaction can be exchanged by *trans*-thiocarbamoylation [12] (Scheme 2.a). Trans-thiocarbamoylation processes can take place either by associative or dissociative bond exchange mechanisms [11,31,32]. The network structure is preserved after reprocessing under suitable conditions [11,31], and repeated reprocessing ability is possible [12].

The bonds produced by the thiol-epoxy reaction are capable of undergoing several exchange processes. Transesterification reactions (Scheme 2.b) are possible because of the presence of hydroxyl groups produced by the thiol-epoxy reaction and the ester groups coming from structure of the thiol crosslinker [10,33]. Moreover, it is also possible that hydroxyl groups displace the thiol groups in thio-urethane bonds (Scheme 2.c), transforming thio-urethane bonds into urethane bonds [11]. Both reactions will produce changes in the way the bonds are connected within the network structure, in a similar way to transesterification reactions of β-hydroxyester structures in epoxy-carboxylic acid thermosets [9,34]. This is bound to alter the network structure of the material, producing a change in the thermal–mechanical properties of the reprocessed materials, and on subsequent reprocessing capabilities [22]. Finally, dynamic thiol-Michael exchange is also possible (Scheme 2.d) [35,36]. It should be noted that this dynamic process would be present in thiol-epoxy thermosets based on mercaptopropionate derivatives, but such possibility was not considered in previous reports [10,33]. Unlike the other processes, the dynamic thiol-Michael exchange is not expected to produce any change in the network structure.

Within the polymer network, the different possible bond exchange processes may take place at the different rates and therefore may or may not be relevant depending on the temperature. Trans-thiocarbamoylation reactions take place quite fast and at moderate temperatures [11,31]. In contrast, transesterification reactions in thiol-epoxy networks are known to proceed much at a much slower rate and higher temperatures [10,33]. Dynamic thiol-Michael reactions have been reported to proceed and reach equilibrium after several hours at moderate temperatures using model compounds [35,36]. Self-healing capabilities have been reported for lightly crosslinked elastomers [35,37], but healing effectiveness drops significantly with increasing crosslinking density [35]. The rate of the exchange reaction depends also on the presence of electron-withdrawing or electron-donating groups [36]. Given that the materials studied in this work will have a densely crosslinked network structure, it is hypothesized that the rate of the dynamic thiol-Michael reaction will also proceed at a lower rate than the *trans*-thiocarbamoylation reaction.

In consequence, it will be assumed that the bond exchange rate of the *trans*-thiocarbamoylation reaction will be significantly faster than that of the remaining processes. All the remaining, slower bond exchange reactions will depend on the presence of the bonds formed by the thiol-epoxy reaction, and therefore will be treated as a group. We have recently modeled the stress relaxation dynamics of networks containing bonds with different kinetics of bond exchange, showing complex relaxation profiles depending on the network architecture and the relative rate of the bond exchange processes [22]. It is quite apparent that the scenario in the present work could be appropriately described using this complex theoretical approach. However, if all the exchange reactions other than *trans*-thiocarbamoylation have neglible rate, the thiol-epoxy bonds can be treated, from a practical perspective, as permanent bonds [22] at moderate temperatures. In that case, a simpler modelling approach, considering only dynamic thio-urethane bonds, would suffice.

The effect of permanent bonds in the stress relaxation process was first analyzed by Li et al. [10]. This effect can be interpreted by analogy with a network decrosslinking process [22]. The exchange of dynamic bonds implies there is a cleavage and formation of new bonds. This, in turn, implies that the network structure is not altered, but the newly formed bonds will not contribute to the elastic response of the material. From a practical point of view, this is equivalent to assuming that they are permanently cleaved [22]. Once all the dynamic bonds have been

Table 1
Composition (weight fraction of each component, %) of the different formulations prepared in this work. All formulations contained 0.1 phr of MI and 0.1 phr of BG-TBD.

Formulation	r_{NCO}	S3	S4	DG	HDI	IPDI
S3-HDI-1	1	61.24	0	0	38.76	0
S3-HDI-0.75	0.75	55.71	0	17.84	26.45	0
S3-HDI-0.5	0.5	51.10	0	32.73	16.17	0
S3-HDI-0.25	0.25	47.19	0	45.34	7.47	0
S3-HDI-0.125	0.125	45.45	0	50.95	3.60	0
S3-IPDI-1	1	54.45	0	0	0	45.55
S3-IPDI-0.75	0.75	51.34	0	16.44	0	32.22
S3-IPDI-0.65	0.65	50.20	0	22.50	0	27.30
S3-IPDI-0.5	0.5	48.57	0	31.11	0	20.32
S3-IPDI-0.35	0.35	47.04	0	39.18	0	13.78
S3-IPDI-0.25	0.25	46.08	0	44.28	0	9.64
S3-DG-1	1	43.84	0	56.16	0	0
S4-HDI-0.5	0.5	0	49.00	34.13	16.87	0
S4-HDI-0.25	0.25	0	45.11	47.13	7.76	0

cleaved, the remaining structure constituted by the permanent bonds has to be examined. The possible scenarios are illustrated in Fig. 1, where the exchanged bonds are represented as dashed red lines. The exchange of bonds leads to the additional deactivation of other bonds that have not been exchanged (solid blue lines), which also lose elastic activity, because they are partially or completely disconnected from the network structure; in a real decrosslinking process, they would be equivalent to fractions of soluble material or dangling chains. The point at which the stress relaxes completely is also equivalent to degelation, the disintegration of the network structure. Following this analogy, it can be deduced that it is not necessary for all the bonds in the network to be exchanged in order to relax the stress completely (Fig. 1.a). However, if the contribution of dynamic exchangeable bonds is not sufficient, a percolated permanent network structure will result with remaining elastic activity (thick solid green lines) which will inhibit complete stress relaxation (Fig. 1.b). A theoretical threshold ratio of permanent/dynamic bonds enabling complete stress relaxation can be calculated [10,15,22].

The network decrosslinking analogy makes it possible to model the effect of permanent bonds using well-established recursive network structure analysis methods [1,38,39]. Such modeling approach was recently used by Konuray et al [15,22]. In this work we use a similar method, adapted to the present curing system, which will allow us to determine (a) the limiting threshold of dynamic thio-urethane bonds ensuring complete stress relaxation, (b) the extent of bond exchange required for complete stress relaxation, and (c) the fraction of residual stress when stress relaxation cannot be completed.

The materials analyzed in this work are prepared using commercially available thiol crosslinking agents, diisocyanates and an epoxy resin. A latent thermal catalyst that releases a strong base upon heating [31] is used for both dynamic exchange reactions. The curing kinetics of the materials are analyzed by dynamic scanning calorimetry (DSC). The thermal–mechanical properties of the materials are characterized using dynamic-mechanic analysis (DMA) and DSC. The bond exchange dynamics are studied by stress relaxation experiments in DMA. The thermal stability of the materials is determined using thermogravimetric analysis (TGA). Recycling capabilities are tested by hot press molding of ground materials. The effect of the composition and network architecture on the thermal–mechanical properties, the thermal stability, the stress relaxation dynamics and the recycling/reprocessing capabilities are analyzed. The results are interpreted in the light of the predictions made using the theoretical structural model developed.

2. Materials and methods

2.1. Materials

Trimethylolpropane tris(3-mercaptopropionate) (S3) (M_w = 398.56 g/mol), pentaerythritol tetrakis(3-mercaptopropionate) (S4) (M_w = 488.66 g/mol), bisphenol A diglycidyl ether (DG) (M_w = 340.41 g/mol), hexamethylene diisocyanate (HDI) (M_w = 168.19 g/mol), isophorone diisocyanate (IPDI) (M_w = 222.28 g/mol), 1,5,7-Triazabicyclo[4.4.0] dec-5-ene (TBD), sodium tetraphenylborate and 1-methylimidazole (MI) were provided by Sigma-Aldrich (Merck KGaA, Darmestat, Germany). A latent base generator (BG-TBD) [40] was prepared from TBD and sodium tetraphenylborate following the procedures reported in the literature [13,28,31].

Different familes of materials were prepared using the different isocyanates, namely S3-IPDI-x and S3-HDI-x, where × refers to the molar ratio of isocyanate groups with respect to the thiol groups r_{NCO} (conversely, the molar ratio of epoxy groups with respect to the thiol is equal to 1-*x*). A material without isocyanate, S3-DG-1, was also prepared. Formulations based on tetrafunctional thiol (S4) and HDI, S4-HDI-x, were also prepared. 0.1 phr of MI and 0.1 phr of BG-TBD (calculated with respect to the total formulation mass) were added to the thiol crosslinker and the mixture was homogenized by magnetic stirring at ca 80–90 °C to obtain a homogeneous solution. Next, DG was added to the mixture and was mixed by hand for about 2 min. The isocyanates were lastly added to the solution depending on the type of system and the required ratio. For isocyanate ratios higher than 0.5, an ice bath was required to control the temperature of the mixture due to the fast reaction of thiol and isocyanate groups. The compositions of all formulations are given in Table 1.

Mixtures were injected in a rectangular mold of 20 × 5 × 1 mm using a syringe immediately after mixing the required diisocyanate and homogenizing by hand stirring. The mold was introduced into a preheated oven at 75 °C and left at that temperature for about 2 h to complete the first curing step. In order to complete the second curing step, the mixture was left in the oven for 5 more hours at 140 °C.

2.2. Techniques

2.2.1. Differential scanning calorimetry (DSC)

A Mettler DSC3 + was used to analyze the nonisothermal curing kinetics of the different mixtures. Samples of the uncured liquid formulation about 12 mg in weight were into aluminium pans with pierced lids and analyzed at 10 K/min from −25 to 250 °C. A second dynamic scan was performed at 10 K/min in order to determine the T_g of the cured material. The evolution of the T_g of cured samples were analyzed isothermally keeping the samples at a constant temperature of 140 °C or 180 °C followed by a measurement of the T_g at 10 K/min. This procedure was repeated several times for each sample, with increasing isothermal treatment, in order to obtain the cumulative effect of the thermal treatment on the T_g. All the experiments were performed under a nitrogen purge of 50 mL/min.

2.2.2. Thermogravimetric analysis (TGA)

A thermogravimetric analyzer (TGA) TGA/DSC (Mettler Toledo TGA/DSC1 Greifensee, Switzerland) was used to study the thermal stability of the materials. Nonisothermal tests were carried out at 10 K/min from- 30 to 600 °C. Isothermal tests were also carried out at 140 °C or 180 °C for 12 h, after a preheating at 20 K/min to the desired temperature. All experiments were performed under a nitrogen purge of 50 mL/min.

2.2.3. Dynamic-mechanic analysis (DMA)

The stress-relaxation tests were carried out in a TA Instruments DMA Q800 analyzer (New Castle, DE, USA). Cured samples of 1 mm thickness and 12 mm width were analyzed using a 3-point bending clamp with a

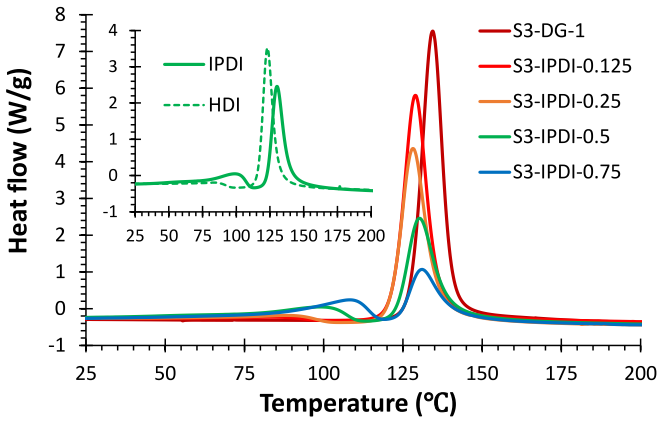

Fig. 2. DSC thermograms of the nonisothermal curing of S3-IPDI-x systems at 10 K/min. The inset compares the thermograms of the S3-IPDI-0.5 and S3-HDI-0.5 systems.

free length of 20 mm at temperatures between 130 and 180 °C. A preload force of 0.002 N was used. The samples were preheated at 10 K/min, the temperature was stabilized and maintainted for 5 min prior to analysis. A constant strain of 1% was applied to measure the stress relaxation. The resulting curves were normalized with respect to the initial value of stress.

2.2.4. Hot pressing

The recycled samples were obtained by cutting the original samples into pieces of ca. 1x1 mm and hot-pressing in an aluminum mold using a Specac Atlas manual 15 T hydraulic hot-press at temperatures of 140 and 180 °C under 10 MPa of pressure.

2.3. Theoretical analysis of stress relaxation

The stress relaxation capabilities were analyzed using a model based on structural fragments, analogous to a network decrosslinking process by assuming the dynamic bonds are broken. Assuming that the transesterification and dynamic thiol-Michael bond exchange processes are much slower than the *trans*-thiocarbamoylation at moderate temperatures, it can be argued that the thiol-epoxy bonds are acting as *de facto* permanent bonds.

Reacted thiol monomers leads to structural fragments with (-) bonds in the network structure, that are connected to (+) bonds from structural fragments of reacted diisocyanate and diepoxy monomers. The bond exchange/decrosslinking process leads to a change in the total number of (-) or (+) bonds from the thiol and isocyanate species, and therefore to a new distribution of connected structural fragments. Relevant structural averages are obtained by defining the probability of capturing the (-) or (+) bonds of the different fragments (in a supposed "fishing" process [1]) and the concepts of expected weight and extinction probabilities of the different bonds (see Appendix A for details).

A threshold molar ratio of isocyanate groups with respect to the thiol groups can be defined, $r_{NCO}{}^{*}$, above which full stress relaxation is possible relying only on the *trans*-thiocarbamoylation bond exchange process. For this scenario of full stress relaxation, $r_{NCO} \geq r_{NCO}{}^{*}$, the extent of bond exchange for complete relaxation x^{*} and the critical ratio $r_{NCO}{}^{*}$ (determined as $x^{*} = 1$) can be easily calculated (see Appendix A for details).

For the trifunctional crosslinker:

$$x^{*} = 1 - \sqrt{1 - \frac{1}{2 \cdot r_{NCO}}} \qquad r_{NCO}{}^{*} = 1/2 \tag{1}$$

For the tetrafunctional crosslinker:

$$x^{*} = 1 - \sqrt{1 - \frac{2}{3 \cdot r_{NCO}}} \qquad r_{NCO}{}^{*} = 2/3 \tag{2}$$

On the other hand, for ratios $r_{NCO} < r_{NCO}{}^{*}$, the fraction of permanent bonds from the thiol-epoxy reaction is prohibitively high for full stress relaxation. Assuming that all the dynamic bonds are exchanged/cleaved, a theoretical fraction of residual stress σ^{*}/σ_0 can be calculated using the expressions in Appendix A. For a trifunctional thiol crosslinker:

$$\sigma^{*}/\sigma_0 = (1 - r_{NCO})^3 \cdot \left(1 - Z^{(-)}\right)^3 \tag{3}$$

and for a tetrafunctional crosslinker:

$$\begin{aligned} \sigma^{*}/\sigma_0 = &(1 - r_{NCO})^4 \cdot \left[\left(1 - Z^{(-)}\right)^4 + 2 \cdot \left(1 - Z^{(-)}\right)^3 \cdot Z^{(-)}\right] \\ &+ (1 - r_{NCO})^3 \cdot (r_{NCO}) \cdot \left[2 \cdot \left(1 - Z^{(-)}\right)^3\right] \end{aligned} \tag{4}$$

In these expressions, $Z^{(-)}$ is the extinction probability of the (-) bonds, determined from the definitions presented in Appendix A. By making use of the phantom network model [1,41], the expressions for σ^{*}/σ_0 also take into consideration the effective elastic contribution of the different crosslinks, which depends on the degree of connectivity of the different fragments involved.

The experimental stress relaxation curves can be fitted to stretched exponential functions [11]:

$$\sigma/\sigma_0 = \sigma^{*}/\sigma_0 + (1 - \sigma^{*}/\sigma_0) \cdot \exp\left(-\left(\frac{t}{\tau}\right)^{\beta}\right) \tag{5}$$

where τ is a characteristic relaxation time determined from the condition $\sigma/\sigma_0 = \sigma^{*}/\sigma_0 + (1 - \sigma^{*}/\sigma_0) \cdot \exp(-1)$. In the absence of permanent network, $\sigma^{*} = 0$, and the condition becomes $\sigma/\sigma_0 \simeq 0.37$.

The activation energy E of the bond exchange process can be determined from the values of τ obtained at different temperatures T and using the following Arrhenius-type equation

$$\ln\tau = \ln A + \frac{E}{R \cdot T} \tag{6}$$

where R is the gas constant and A is a pre-exponential factor.

3. Results

3.1. Differential scanning calorimetry (DSC)

Fig. 2 shows the DSC thermograms of the curing at 10 K/min of the S3-IPDI-x formulations. Two clear curing exotherms are observed, evidencing that the curing process takes place in two well-defined stages with controlled sequence: the thiol-isocyanate reaction followed by the thiol-epoxy reaction. This result corroborates the previous data reported by Gamardella et al. [27]. Across the formulations, the change in the size of the peaks agrees well with the change in the ratio of isocyanate and epoxy groups. When HDI is used (see dashed line in Fig. 2 inset) the first peak is hardly appreciated in comparison with IPDI (solid line) due to the fast kinetics of the thiol-isocyanate reaction, which made it proceed to a significant extent of conversion prior to analysis. The values of the reaction enthalpy corresponding to each curing system are reported in Table 2. The enthalpy of reaction of the thiol-isocyanate reaction could not be measured when HDI was used, while values around 40–60 kJ/eq could be determined when IPDI was used; the values are comparable to those reported by Gamardella et al. for a similar dual-curing system based on a tetrathiol crosslinker [27]. In all cases, the reaction enthalpy of the thiol-epoxy reaction was about 120 kJ/eq, which is similar to the typical values reported for thiol-epoxy reactions [42] and for similar dual-curing systems [27].

The T_g of the fully cured IPDI samples shown in Table 2 evidence a strong decrease in T_g when more epoxy is used, starting from a very high

Table 2
Results of the calorimetric analysis of the different formulations. Undetermined values are marked as (-).

Formulation	$\Delta h_1(J/g)$	$\Delta h_1(kJ/eq)$	$\Delta h_2(J/g)$	$\Delta h_2(kJ/eq)$	T_g(°C)	$T_{g,FOX}$(°C)
S3-HDI-1	–	–	–	–	41.5	41.5
S3-HDI-0.75	–	–	–	–	39.0	39.7
S3-HDI-0.50	–	–	235	122	38.0	38.3
S3-HDI-0.25	–	–	290	109	38.0	37
S3-HDI-0.125	–	–	390	130	37.0	36.5
S3-IPDI-1	–	–	–	–	112	112
S3-IPDI-0.75	121	42	123	128	75.0	86.1
S3-IPDI-0.5	96	53	217	119	64.0	65.8
S3-IPDI-0.25	31	36	316	121	45.0	49.5
S3-IPDI-0.125	27	64	389	131	41.5	42.4
S3-IPDI-0	–	–	458	119	36.0	36.0

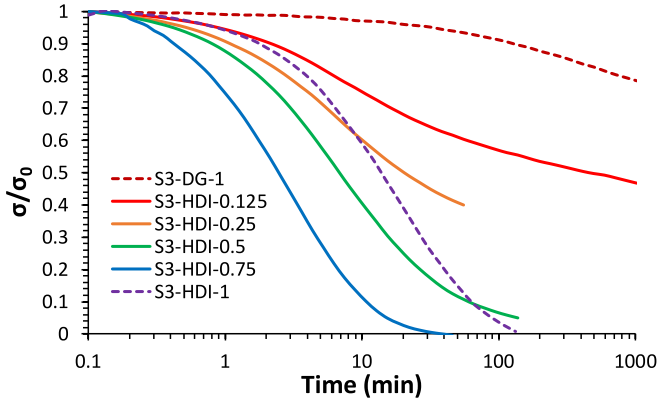

Fig. 3. Stress relaxation of HDI formulations at 140 °C.

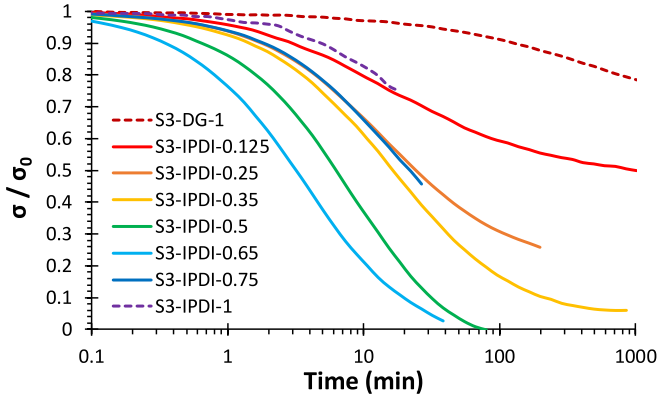

Fig. 4. Stress relaxation of IPDI formulations at 140 °C.

Table 3
Results of the stress relaxation of S3-HDI-x and S3-IPDI-x systems at 140 °C. Experimental curves were fitted to equation (5).

Formulation	r_{NCO}	σ^*/σ_0	$\tau(min)$	β
S3-HDI-1	1	0.034	20.4	0.89
S3-HDI-0.75	0.75	0.019	3.78	0.97
S3-HDI-0.50	0.5	0.087	9.33	0.84
S3-HDI-0.25	0.25	0.420	8,25	0.82
S3-HDI-0.125	0.125	0.519	17.1	0.70
S3-IPDI-0.75	0.75	0.062	4.5	0.825
S3-IDI-0.50	0.5	0.020	9.6	0.823
S3-IPDI-0.35	0.35	0.081	23.6	0.736
S3-IPDI-0.25	0.25	0.295	18.0	0.80
S3-IPDI-0.125	0.125	0.518	28.9	0.62

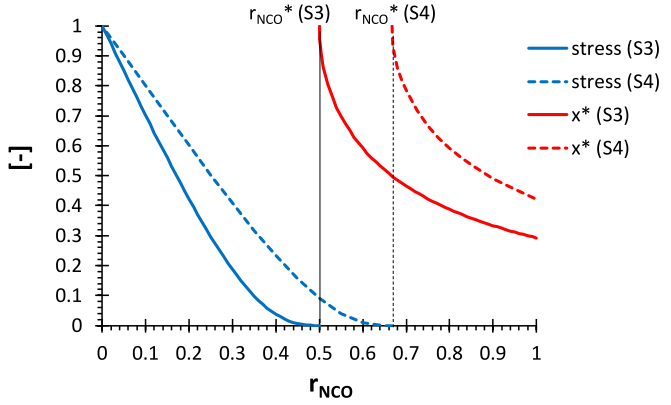

Fig. 5. Theoretical prediction of the residual stress (σ^*/σ_0) with $r_{NCO} < r_{NCO}^*$ and the theoretical extent of bond exchange (x^*) in materials with $r_{NCO} \geq r_{NCO}^*$, for materials crosslinked using trifunctional thiol (S3) and tetrafunctional thiol (S4), determined using the expressions in section 2.3 and the Appendix. The thin black lines represent the threshold ratio of isocyanate groups, r_{NCO}^*.

value of 112 °C for the pure S3-IPDI-1. In contrast, all the samples with HDI show T_g ranging from 36 to 42 °C with a slightly decreasing trend with increasing epoxy content. The effect of the composition on the final properties of the materials is comparable to that observed by Gamardella et al. for similar dual-curing systems [27]. Indeed, it can be checked (see Table 2) that the T_g of the different materials can be reasonably predicted as a mixture of thiol-isocyanate and thiol-epoxy networks by the Fox equation

$$\frac{1}{T_{g,FOX}} = \frac{w_1}{T_{g,1}} + \frac{w_2}{T_{g,2}} \tag{7}$$

where w_1 and $w_2 = 1 - w_1$ are the weight fraction of the thiol-isocyanate and thiol-epoxy components in the mixed system respectively; $T_{g,1}$ and $T_{g,2}$ are the glass transition temperatures of the pure thiol-isocyanate and thiol-epoxy networks respectively.

It is deemed that the values of T_g of the HDI formulations are sufficiently low to permit sufficient segmental mobility of the network so as not to affect the kinetics of the relaxation process. IPDI-rich materials (especially S3-IPDI-1) have significantly higher T_g, which suggests the mobility might potentially be hindered if the temperature is not sufficiently high.

3.2. Dynamic mechanical analysis

The stress relaxation of the different materials was analyzed at 140 °C using DMA. The results for the formulations with HDI are shown in Fig. 3 and those with IPDI are shown in Fig. 4. In both cases, highly interesting trends are reported with respect to the ratio of isocyanate (r_{NCO}) in each material. Table 3 summarizes the results of the analysis of

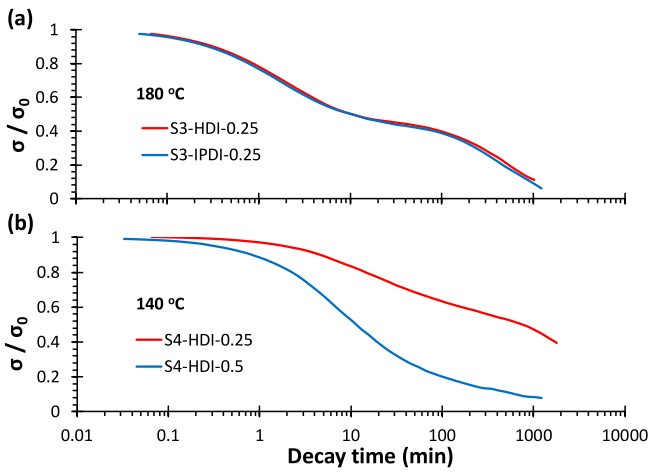

Fig. 6. (a) Stress relaxation at 180 °C of S3-HDI-0.25 and S3-IPDI-0.25 materials. (b) Stress relaxation at 140 °C of S4-HDI-0.25 and S4-HDI-0.5 materials.

the stress relaxation curves in Fig. 3 and Fig. 4.

To begin with, the stress relaxation of the pure HDI formulation takes place within ca. 100 min, a result that is very similar to that reported by Gamardella et al. [31]. However, it can be observed that, when 25% epoxy is used (S3-HDI-0.75, Fig. 3, blue curve), the relaxation process is considerably faster. Nevertheless, further increase in epoxy content leads to slower relaxation, with full relaxation only possible up to an epoxy content of 50 % (S3-HDI-0.5). At epoxy contents of 75% (S3-HDI-0.25) and 87.5% (S3-HDI-0.125), a fraction of unrelaxed stress is clearly observed, increasing with the epoxy content. Moreover, the relaxation processes become increasingly broader and slower with increasing epoxy content. A remarkable difference between the pure epoxy network, S3-DG-1, and the fastest thiourethane network, S3-HDI-0.75, is observed, suggesting that the ester bonds in the network structure play a role akin to permanent bonds. Similar results are shown in Fig. 4 for materials based on IPDI. Noticeably, the relaxation of the 100 % IPDI material (S3-IPDI-1) is extremely slow, with comparable kinetics to that of 87.5% DG. This is not unexpected, since the T_g of S3-IPDI-1 is only about 30 °C lower than the test temperature.

Knowing that the *trans*-thiocarbamoylation is considerably faster than the other processes shown in Scheme 2, it can be assumed that the bonds formed by thiol-isocyanate reaction are dynamic, while those coming from the thiol-epoxy reaction act as permanent bonds at the

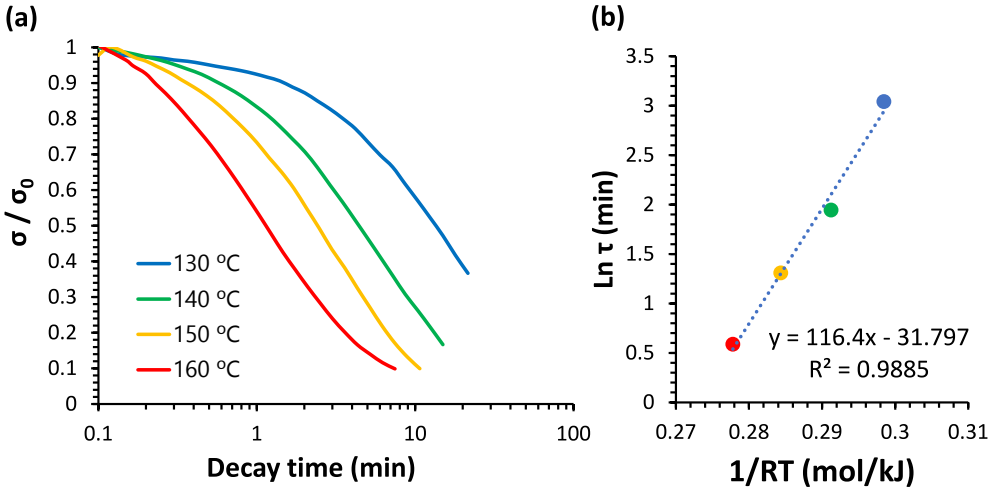

Fig. 7. (a) Normalized stress-relaxation plot as a function of time at different temperatures for S3-HDI-0.75 formulation, from 130 to 160 °C (b) Arrhenius plot of the logarithmic relaxation times against the inverse of temperature.

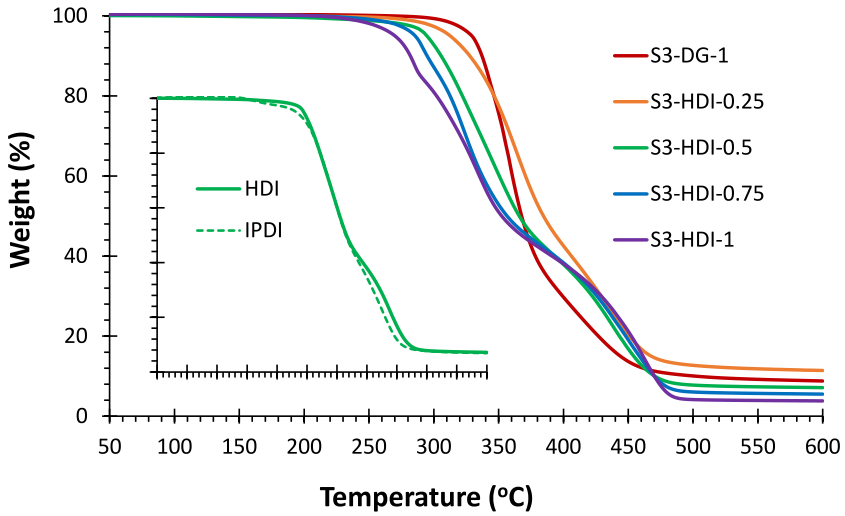

Fig. 8. Results of TGA analysis of at 10 K/min of S3-HDI-x materials. The inset compares S3-HDI-0.5 and S3-IPDI-0.5 materials.

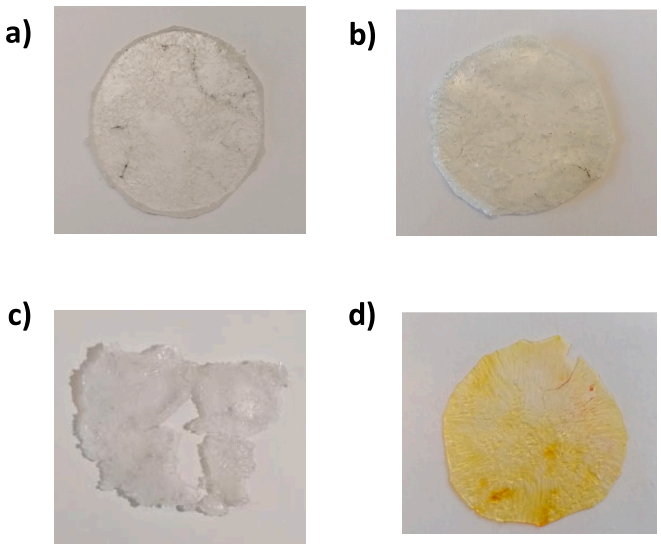

Fig. 9. Photographs showing the results of the hot press molding of a) S3-HDI-0.5 at 140 °C under 10 MPa pressure for 5 h, b) S3-IPDI-0.65 at 140 °C under 10 MPa pressure for 3 h, c) S3-IPDI-0.25 at 140 °C under 10 MPa pressure for 4 h, and d) S3-IPDI-0.25 at 180 °C under 10 MPa pressure for 4 h.

temperature of analysis. Based on this hypothesis, it is possible to make some theoretical predictions of the expected relaxation behavior using the expressions in section 2.3 and in Appendix A. The results of these predictive calculations are given in Fig. 5.

Considering that a trifunctional thiol crosslinker was used, a threshold ratio of isocyanate:thiol groups in the mixture for complete stress relaxation can be calculated as $r_{NCO}^{*} = 0.5$ (equation (1)). Within experimental error, it is verified that stress relaxation is complete for all materials with $r_{NCO} \geq r_{NCO}^{*}$. This confirms the possibility of having a controlled non-zero fraction of permanent bonds in the network structure without jeopardizing full reprocessing capability [10].

Above the threshold ratio, $r_{NCO} \geq r_{NCO}^{*}$, stress relaxation is complete but the fraction of bond exchange required to relax the network, x^{*}, increases with decreasing isocyanate content. In the absence of any other effects, an increase in x^{*} would result in a longer process from a kinetic perspective, and therefore it would be expected to produce an increase in the relaxation time τ. The relaxation data shown in Fig. 3 and Table 3 for the HDI materials show that the relaxation of the S3-HDI-0.75 material is in fact faster than that of the S3-HDI-1 material, but then there is a regular increase of the relaxation time with decreasing HDI content, in agreement with the predicted theoretical behavior. This seems to indicate that either the presence of DG or else the bonds formed in the thiol-epoxy reaction contribute to activate the bond exchange catalyst, the latent base BG-TBD. A similar effect is observed for IPDI (see Fig. 4 and Table 3), but in this case it is evidenced that the stress relaxation of S3-IPDI-1 material is much slower. As was mentioned previously, this can be rationalized by the high T_g of the material of 112 °C, which is only slightly below the relaxation temperature of 140 °C. Under these conditions, the reduced segmental mobility of the network is expected to impede the relaxation process significantly [7], in addition to other side chemical effects.

Below this threshold ratio, $r_{NCO} < r_{NCO}^{*}$, the fraction of permanent bonds in the network, coming from the thiol-epoxy reaction, leads to the presence of a permanent network structure resulting in an incomplete relaxation of the stress. The fraction increases with decreasing isocyanate content. In this region, permanent creep is minimized or avoided and reprocessing capabilities would be limited [10]. The predicted residual stress σ^{*}/σ_0 shown in Fig. 5 agrees well with the results presented in Table 3. It is also observed that decreasing r_{NCO} generally leads to an increase in relaxation time. The results in Fig. 5 also suggest that quantitative stress relaxation would be possible at r_{NCO} slightly below r_{NCO}^{*}. This indicates that some interesting reprocessing capabilities such as reshapeability in combination with creep suppression would be retained.

Table 3 also shows the values of the shape parameter β. All the values are lower than 1, as can be expected taking into consideration the results reported by other authors [10,11,33,43]. It is also observed that the value of β decreases with increasing contribution of the permanent (or slow-relaxing) component, which indicates a broadening ot the stress relaxation process, in agreement with the results of Li et al [10].

Overall, the experimental results confirm that quantitative and qualitative predictions can be made using a simplified structural model, by considering the presence of permanent bonds in the network structure, and therefore evidence the possibility of designing vitrimers with tunable relaxation behavior. However, it is observed that the stress does not reach a plateau value in maerials with $r_{NCO} < r_{NCO}^{*}$, but that it continues to decrease. This is attributed to the additional but slower bond exchange reactions taking place (see Scheme 2). In order to confirm the existence of the second relaxation process, stress relaxation experiments were carried out at a temperature of 180 °C. Fig. 6(a) shows that both S3-HDI-0.25 and S3-IPDI-0.25, which were unable to relax completely at 140 °C within a reasonable timescale, exhibit an apparent two-step relaxation profile that is related to the co-occurrence of the *trans*-thiocarbamoylation (1st step), and the aforementioned additional exchange reactions (2nd step). This behavior is similar to the one reported recently for some thiol-ene materials [15] and it corroborates the predictions that can be made using more complex theoretical approaches [22].

According to the theoretical analysis of the permanent network and the predictions shown in Fig. 5, the use of a higher functional crosslinker leads to a network with higher permanent fraction. When a

Table A2
Distribution of dg (diepoxy) and $I-b$ (diisocyanate) fragments, (+) bonds and capture probabilities for a trifunctional thiol crosslinker.

Fragment	Number of fragments	Number of (+) bonds	$\mathbf{p}_i^{(+)}$
DG	$\frac{3}{2}\cdot(1-r_{NCO})$	$3\cdot(1-r_{NCO})$	$\frac{1-r_{NCO}}{1-r_{NCO}\cdot x}$
I-2	$\frac{3}{2}\cdot r_{NCO}\cdot(1-x)^2$	$3\cdot r_{NCO}\cdot(1-x)^2$	$\frac{r_{NCO}\cdot(1-x)^2}{1-r_{NCO}\cdot x}$
I-1	$\frac{3}{2}\cdot r_{NCO}\cdot 2\cdot(1-x)\cdot x$	$3\cdot r_{NCO}\cdot(1-x)\cdot x$	$\frac{r_{NCO}\cdot(1-x)\cdot x}{1-r_{NCO}\cdot x}$
I-0	$\frac{3}{2}\cdot r_{NCO}\cdot x^2$	0	0
Total	3/2	$3\cdot(1-r_{NCO}\cdot x)$	1

Table A1
Distribution of $S-a$ fragments for a trifunctional thiol, (-) bonds and capture probabilities.

Fragment	Number of fragments	Number of (-) bonds	$P_i^{(-)}$
S-3	$(1-r_{NCO}\cdot x)^3$	$3\cdot(1-r_{NCO}\cdot x)^3$	$(1-r_{NCO}\cdot x)^2$
S-2	$3\cdot(1-r_{NCO}\cdot x)^2\cdot(r_{NCO}\cdot x)$	$6\cdot(1-r_{NCO}\cdot x)^2\cdot(r_{NCO}\cdot x)$	$2\cdot(1-r_{NCO}\cdot x)\cdot(r_{NCO}\cdot x)$
S-1	$3\cdot(1-r_{NCO}\cdot x)\cdot(r_{NCO}\cdot x)^2$	$3\cdot(1-r_{NCO}\cdot x)\cdot(r_{NCO}\cdot x)^2$	$(r_{NCO}\cdot x)^2$
S-0	$(r_{NCO}\cdot x)^3$	0	0
Total	1	$3\cdot(1-r_{NCO}\cdot x)$	1

Table A3
Distribution of $S-a$ fragments for a tetrafunctional thiol, (-) bonds and capture probabilities.

Fragment	Number of fragments	Number of (-) bonds	$P_i^{(-)}$
S-4	$(1-r_{NCO}\cdot x)^4$	$4\cdot(1-r_{NCO}\cdot x)^4$	$(1-r_{NCO}\cdot x)^3$
S-3	$4\cdot(1-r_{NCO}\cdot x)^3\cdot(r_{NCO}\cdot x)$	$12\cdot(1-r_{NCO}\cdot x)^3\cdot(r_{NCO}\cdot x)$	$3\cdot(1-r_{NCO}\cdot x)^2\cdot(r_{NCO}\cdot x)$
S-2	$6\cdot(1-r_{NCO}\cdot x)^2\cdot(r_{NCO}\cdot x)^2$	$12\cdot(1-r_{NCO}\cdot x)^2\cdot(r_{NCO}\cdot x)^2$	$3\cdot(1-r_{NCO}\cdot x)\cdot(r_{NCO}\cdot x)^2$
S-1	$4\cdot(1-r_{NCO}\cdot x)\cdot(r_{NCO}\cdot x)^3$	$4\cdot(1-r_{NCO}\cdot x)\cdot(r_{NCO}\cdot x)^3$	$(r_{NCO}\cdot x)^3$
S-0	$(r_{NCO}\cdot x)^4$	0	0
Total	1	$4\cdot(1-r_{NCO}\cdot x)$	1

tetrafunctional thiol crosslinker is used, the theoretical threshold ratio $r_{NCO}{}^*$ is calculated as 0.67 (equation (2)), which is higher than the case when the trifunctional thiol crosslinker is used. In addition, for a given value of $r_{NCO} > 0$, the value of the residual stress, if any, should be higher. We verified this behavior by analyzing the stress relaxation of materials with HDI using a tetrafunctional thiol crosslinker. In Fig. 6(b) it can be observed that the S4-HDI-0.5 material is unable to relax the stress completely at 140 °C, leaving a residual value around 0.1, because $r_{NCO} < r_{NCO}{}^*$, in contrast with the completely relaxing S3-HDI-0.5, for which $r_{NCO} = r_{NCO}{}^*$ (see Fig. 3). Moreover, the S4-HDI-0.25 shows a residual stress around 0.5, which is considerably higher than that of S3-HDI-0.25 (see Fig. 3). This influence of the crosslinker functionality can also be reasonably predicted using the concept of permanent network, as shown in Fig. 5.

The temperature-dependence of the stress relaxation kinetics was also analyzed. The stress relaxation of S3-HDI-0.75 was analyzed at different temperatures, as seen in Fig. 7. The plot of $\ln\tau$ with respect to the reciprocal T gives a straight line (see inset) with slope equal to the activation energy, evaluated as 116.4 kJ/mol, similar to what was reported by Gamardella et al. for pure HDI systems using a latent base generator [31]. In spite of the strong kinetic effect produced by the use of a mere 25% of epoxy in the material (see Fig. 3), the stress relaxation process appears to be governed by the same *trans*-thiocarbamoylation reaction, which is to be expected considering that the slow-relaxing ester bonds from the thiol-epoxy reaction are in fact acting as permanent bonds and therefore do not participate in the relaxation process.

3.3. Thermal stability

The thermal stability of the different materials was analyzed by TGA and DSC. Fig. 8 shows the results from the analysis of the thermal stability of the HDI materials at 10 K/min. As can be seen the thermal stability increases with increasing amount of epoxy (decreasing isocyanate, r_{NCO}) in the formulation. It can also be observed that the weight loss is almost negligible at the temperatures chosen for the stress relaxation measurements, suggesting that the materials are thermally stable at the reprocessing conditions. If the data of the pure thiol-isocyanate materials are compared with the results published by Gamardella et al. [31], it can be appreciated that the materials prepared in this work have somewhat higher thermal stabilities. The degradation process has multiple steps, the first of which takes place at a higher temperature than that previously reported [31]. This may be explained by the different catalytic activity of TBD, which is a strong base, in comparison with DBU used by Gamardella et al. [31], which is both a strong base and a good nucleophile. The fact that that the thermal stability of the materials containing epoxy is even higher makes these dual-curing materials even safer for reprocessing. The inset shows that the thermal stability of S3-IPDI-0.5 material is only slightly lower than that of S3-HDI-0.5, with an overall comparable thermal degradation profile.

In order to confirm these results, isothermal TGA and DSC tests were carried out in order to determine the weight loss and possible changes in the network structure upon prolonged exposure at 140 °C. It was verified that materials treated at 140 °C showed a weight loss lower than 0.5 % in 12 h, and the T_g were stable, evidencing no change in the network structure (results not shown). Therefore, it can be argued that repeated reprocessing at such moderate temperatures is safe. In addition, it can also be assumed thatthe *trans*-thiocarbamoylation is the only relevant bond exchange process taking place, without changing network structure. The fact that the network structure remains unaltered at 140 °C suggests that the recycling ability would be maintained in successive reprocessing cycles, provided that the catalyst is not being deactivated.

Table A4
Distribution of dg (diepoxy) and $I-b$ (diisocyanate) fragmentss, (+) bonds and capture probabilities for a tetrafunctional thiol crosslinker.

Fragment	Number of fragments	Number of (+) bonds	$P_i^{(+)}$
DG	$2\cdot(1-r_{NCO})$	$4\cdot(1-r_{NCO})$	$\frac{1-r_{NCO}}{1-r_{NCO}\cdot x}$
I-2	$2\cdot r_{NCO}\cdot(1-x)^2$	$4\cdot r_{NCO}\cdot(1-x)^2$	$\frac{r_{NCO}\cdot(1-x)^2}{1-r_{NCO}\cdot x}$
I-1	$2\cdot r_{NCO}\cdot 2\cdot(1-x)\cdot x$	$4\cdot r_{NCO}\cdot(1-x)\cdot x$	$\frac{r_{NCO}\cdot(1-x)\cdot x}{1-r_{NCO}\cdot x}$
I-0	$2\cdot r_{NCO}\cdot x^2$	0	0
Total	2	$4\cdot(1-r_{NCO}\cdot x)$	1

In the case of materials that cannot be fully relaxed at 140 °C, the stability at higher temperatures needs to be examined. For that purpose, S3-HDI-0.25 and S3-IPDI-0.25 materials were treated at 180 °C. They exhibited only moderate weight losses, measured as less than 2 % within the first 1–2 h, after which the weight remained highly stable. The T_g of S3-HDI-0.25 remained constant, at 38 °C, within the first 6 h and only increased from 39 to 41 °C between 8 and 16 h. In the case of the S3-IPDI-0.25 material, a similar behavior was observed: a constant T_g of 42 °C was observed up to 6 h, then T_g increased from 43 to 47 °C between 8 and 16 h. These results confirm that the *trans*-thiocarbamoylation process does not produce any relevant change in the network structure of the materials, while the additional bond exchange processes, if allowed sufficient time, might produce some changes in the network architecture. This is to be expected taking into consideration that the participation of hydroxyl groups from the thiol-epoxy network may change the distribution of bonds in the structural fragments within the network structure, as illustrated in Scheme 2. Indeed, if one compares the thermal stability data and the stress relaxation profiles of S3-HDI-0.25 and S3-IPDI-0.25 at 180 °C (see Fig. 6(a)), it can be observed that a significant fraction of the stress is already relaxed within the first 6–8 h, when changes in the network structure are virtually negligible. This suggests that these materials might also be reprocessed under such conditions with little impact on their thermal and mechanical properties.

3.4. Recycling capabilities

The recyclability and reprocessing capabilities of three materials were studied: two samples with HDI (S3-HDI-0.5 and S3-HDI-0.25) and one with IPDI (S3-IPDI-0.65). Reprocessing time in the hot press was tentatively determined from the stress relaxation test results. All three samples were recycled under 10 MPa pressure. S3-HDI-0.5, which has been formulated with the threshold isocyanate ratio $r_{NCO}{}^* = 0.5$, could be effectively recycled at 140 °C in 5 h (Fig. 9.a). S3-IPDI-0.65 was also

fully recycled at 140 °C in only 3 h with uniform appearance (Fig. 9.b), which is not surprising since $r_{NCO} > r_{NCO}^*$ for this material. As can be seen, it is possible to completely recycle materials despite a significant fraction of permanent (or slow-relaxing bonds). This result is in agreement with previous observations [10,15]. Furthermore, it is evident that theoretical predictions of stress relaxation provide a highly useful input for the determination of the recycling ability of the materials.

By way of contrast, materials with lower isocyanate content, $r_{NCO} < r_{NCO}^*$, could not be efficiently recycled at 140 °C (Fig. 9.c) because of the hindrance by the permanent (slow-relaxing) thiol-epoxy network. However, it was possible to carry out the recycling process at 180 °C with better results (Fig. 9.d), aided by the activation of the additional bond exchange processes within the thiol-epoxy network. Noticeably, it was not needed to relax the network completely in order to reprocess the samples, and only a moderate change in color was observed.

4. Conclusions

We have presented a ternary thermosetting system exploiting both the enhanced processing capabilities of a dual-curing system and the reprocessing capabilities of vitrimer-like materials. A robust control of the curing sequence is guaranteed by the highly selective attack of the thiolate anion to the isocyanate, leading to completion of the first curing reaction in a short time under mild conditions, long before the thiol-epoxy reaction is activated. The adhesion and reshaping capabilities of the intermediate material can be exploited as a means of processing flexibility, thereby widening the scope of applicability of these materials.

It has been shown that it is possible to achieve complete stress relaxation in the presence of a controlled fraction of permanent (or slow-exchanging) bonds in the network structure. This makes it possible to obtain fully recyclable and reprocessable materials without requiring that all the bonds in the network structure are dynamic. Making use of a structural model, we have defined a theoretical threshold of the ratio of isocyanate bonds in the mixture, r_{NCO}^* determining the ability of the network to relax the stress completely. At isocyanate ratios higher than this threshold, $r_{NCO} \geq r_{NCO}^*$, full relaxation is possible because the presence of permanent (or slow-exchanging) bonds is not sufficient to sustain a permanent network structure. Below this ratio, $r_{NCO} < r_{NCO}^*$ stress relaxation is incomplete due to the existence of a permanent network structure, leading to a predictable fraction of residual stress, which limits the reprocessing capabilities of the material. Theoretical calculations are in agreement with experimental results, and as such provide a basis for optimization of experimental conditions in the context of material design. In addition, it would be possible to design fully relaxing networks with a loosely crosslinked permanent network structure without compromising interesting features such as creep suppression capability.

In the design of vitrimers, reducing the dynamic content can be sought after if the dynamic bond exchange components are costly. However, this comes at a price of reduced recyclability because of the higher extent of bond exchange that would be required to relax the network. Exceptionally, in the present work it has been shown that the relaxation of the pure thiol-isocyanate material is slower than that of a material containing a controlled amount of epoxy. This could be due to a chemical interaction which involves the epoxy, that apparently enhances the *trans*-thiocarbamoylation bond exchange process.

The stress relaxation and recycling results are promising the possibility of designing vitrimer materials with tailored network architecture and relaxation behavior, accompanied by the reduced use of harmful isocyanate components. However, to provide further insight in this quest, a number of issues need to be investigated in detail: the effect of the presence of permanent network on reprocessing capabilities such as reshaping, scratch healing, adhesion or recycling by hot compression molding; the effective threshold ratio r_{NCO}^* enabling reprocessing capabilities and the extent to which they may be affected when $r_{NCO} < r_{NCO}^*$; and the optimum reprocessing time required to quantitatively achieve the desired effect. Research is underway to answer some of these questions.

CRediT authorship contribution statement

Sasan Moradi: Formal analysis, Investigation, Writing – original draft. **Xavier Fernández-Francos:** Conceptualization, Methodology, Supervision, Validation, Writing – review & editing. **Osman Konuray:** Conceptualization, Investigation, Methodology, Supervision, Validation, Writing – original draft, Writing – review & editing. **Xavier Ramis:** Conceptualization, Formal analysis, Funding acquisition, Investigation, Methodology, Project administration, Resources, Supervision, Validation, Writing – review & editing.

Declaration of Competing Interest

The authors declare the following financial interests/personal relationships which may be considered as potential competing interests: [Xavier Ramis, Xavier Fernandez-Francos reports financial support and equipment, drugs, or supplies were provided by Spanish Ministry of Science and Innovation.].

Data availability

Data will be made available on request.

Acknowledgements

This work was funded by the Spanish Ministry of Science and Innovation (MCIN/AEI/10.13039/501100011033) through R&D project PID2020-115102RB-C22, and also by Generalitat de Catalunya (2021-SGR-00154), Spain. X. Fernández-Francos and O. Konuray acknowledge the Serra-Húnter programme (Generalitat de Catalunya).

Appendix A

The stress relaxation capabilities were analyzed using a model similar to the one recently developed by Konuray et al [15]. The model treats the effect of the bond exchange process as a network decrosslinking process and is based on the recursive network structure analysis methods of Macosko and Miller [38,39] and Williams et al. [1]. It is assumed that the transesterification and dynamic thiol-Michael bond exchange processes are much slower than the *trans*-thiocarbamoylation, that is, that the thiol-epoxy bonds are acting *de facto* as permanent bonds.

Reacted thiol monomers leads to (-) bonds in the network structure, that are connected to (+) bonds from reacted isocyanate and epoxy monomers. The bond exchange/decrosslinking process leads to a change in the total number of (-) or (+) bonds and to the distribution of connected species. Relevant structural averages are obtained by defining the probability of capturing the (-) or (+) bonds of the different fragments and the concepts of expected weight and extinction probability. Expressions are shown in detail for a material based on a diisocyanate, a diepoxy, and a trifunctional thiol or a tetrafunctional thiol.

Trifunctional thiol crosslinking agent

Taking as a reference 1 mol of trifunctional thiol crosslinker, a distribution of thiol $S-a$ species issuing a non-exchanged (-) bonds can be defined from a binomial distribution as follows:

$$n_{S-a} = \binom{3}{a}\cdot(1 - r_{NCO}\cdot x)^{a}\cdot(r_{NCO}\cdot x)^{3-a} \qquad a = 0,1,2,3 \tag{A1}$$

The number of (-) bonds coming from each fragment is calculated as $a\cdot n_{S-a}$. The capture probabilities of each fragment with (-) bonds, $P_{S-a}^{(-)}$, is calculated as:

$$P_{S-a}^{(-)} = \frac{a\cdot n_{S-a}}{\sum_{a=0}^{3} a\cdot n_{S-a}} \tag{A2}$$

In the above expressions, x is the fractional extent of bond exchange and r_{NCO} is the ratio if isocyanate:thiol groups in the formulation. Notice that at the beginning of the process, $x = 0$, when no dynamic bonds have been exchanged/cleaved, the thiol species is only in the form of $S-3$ (all the bonds are connected). The detailed distribution of species and fragment capture probabilities is shown in Table A1.

We can also define the species with (+) bonds, corresponding to the diepoxy component (DG) and the diisocyanate component (I). Taking as a reference 1 mol of trifunctional thiol, the total amount of diepoxy species is $(3/2)\cdot(1-r_{NCO})$ and that of diisocyanate is $(3/2)\cdot r_{NCO}$. The bond exchange process does not alter the DG component but leads to a a distribution of species from the diisocyanate issuing b bonds, $I-b$.

$$n_{I-b} = (3/2)\cdot r_{NCO}\cdot\binom{2}{b}\cdot(1-x)^{b}\cdot x^{2-b} \qquad b = 0,1,2$$

$$n_{DG} = (3/2)\cdot(1 - r_{NCO}) \tag{A3}$$

The number of (+) bonds coming from each isocyanate fragment is calculated as $b\cdot n_{I-b}$. The number of (+) bonds coming from the DG fragment is $2\cdot n_{DG}$ The capture probabilities of each fragment with (+) bond is calculated as:

$$P_{I-b}^{(+)} = \frac{b\cdot n_{I-b}}{2\cdot n_{DG} + \sum_{b=0}^{2} b\cdot n_{I-b}} \qquad P_{DG}^{(+)} = \frac{2\cdot n_{DG}}{2\cdot n_{DG} + \sum_{b=0}^{2} b\cdot n_{I-b}} \tag{A4}$$

Table A2 summarizes the concentration of the different species, (+) bonds and capture probabilities.

In order to analyze the stress relaxation process, we start with the concept of expected weight pending from (-) and (+) bonds, $W^{(-)}$ and $W^{(+)}$ respectively, which are calculated recursively from the probability of capturing a complementary fragment and the fragment mass plus the expected mass pending from the remaining bond.

$$W^{(-)} = P_{DG}^{(+)}\cdot\left(W^{(+)} + M_{DG}\right) + P_{I-2}^{(+)}\cdot\left(W^{(+)} + M_I\right) + P_{I-1}^{(+)}\cdot M_I$$

$$W^{(+)} = P_{S-3}^{(-)}\cdot\left(2\cdot W^{(-)} + M_S\right) + P_{S-2}^{(-)}\cdot\left(W^{(-)} + M_S\right) + P_{S-1}^{(-)}\cdot M_S \tag{A5}$$

Where M_S, M_{DG} and M_I are the mass of the different $S-a$, DG and $I-b$ fragments. This system of expression is expressed in matrix form as

$$\begin{pmatrix} 1 & a_{-,+} \\ a_{+,-} & 1 \end{pmatrix}\cdot\begin{pmatrix} W^{(-)} \\ W^{(+)} \end{pmatrix} = \begin{pmatrix} I^{(-)} \\ I^{(+)} \end{pmatrix} \tag{A6}$$

Where.

$$a_{-,+} = -P_{DG}^{(+)} - P_{I-2}^{(+)} = -\left(\frac{1 - r_{NCO} + r_{NCO}\cdot(1-x)^2}{1 - r_{NCO}\cdot x}\right)$$

$$a_{+,-} = -2\cdot P_{S-3}^{(-)} - P_{S-2}^{(-)} = -2\cdot(1 - r_{NCO}\cdot x)^2 - 2\cdot(1 - r_{NCO}\cdot x)\cdot(r_{NCO}\cdot x) = -2\cdot(1 - r_{NCO}\cdot x) \tag{A7}$$

Complete stress relaxation takes place at a given $x = x^{*} < 1$. This occurs when the determinant of the matrix of coefficients is equal to 0, $1 - a_{-,+}\cdot a_{+,-} = 0$. If the values of the different coefficients are replaced in the expression, we reach:

$$1 - \left(\frac{1 - r_{NCO} + r_{NCO}\cdot(1-x)^2}{1 - r_{NCO}\cdot x}\right)\cdot 2\cdot(1 - r_{NCO}\cdot x) = 0$$

$$1 - 2\cdot\left(1 - r_{NCO} + r_{NCO}\cdot(1-x)^2\right) = 0$$

$$x = x^{*} = 1 - \sqrt{1 - \frac{1}{2\cdot r_{NCO}}} \tag{A8}$$

This expression only has solution when $r_{NCO} \geq r_{NCO}{}^{*} = 1/2$. It follows that full stress relaxation is only possible ($x^{*} < 1$) for materials with $r_{NCO} \geq r_{NCO}{}^{*}$, that is, when the fraction of dynamic bonds in the network is sufficiently high.

When $r_{NCO} < r_{NCO}{}^{*}$ stress relaxation is not complete and a residual stress is obtained at the end of the process, when $x = 1$. In order to determine this residual stress, it is necessary to use the concept of extinction probabilities, that is, the probability that a given bond has a finite continuation. The extinction probabilities of the (-) and (+) bonds, $Z^{(-)}$ and $Z^{(+)}$ respectively, are calculated recursively from the probability of capturing complementary fragments and the extinction probability of the fragments, taking into consideration the remaining bonds:

$$Z^{(-)} = P_{DG}^{(+)}\cdot Z^{(+)} + P_{I-2}^{(+)}\cdot Z^{(+)} + P_{I-1}^{(+)}$$

$$Z^{(+)} = P_{S-3}^{(-)}\cdot\left(Z^{(-)}\right)^2 + P_{S-2}^{(-)}\cdot Z^{(-)} + P_{S-1}^{(-)} \tag{A9}$$

By considering that $x = 1$ in the expressions of the capture probabilities, this yields a simple expression:

$$Z^{(-)} = Z^{(+)}$$

$$Z^{(+)} = \left[(1 - r_{NCO})\cdot Z^{(-)} + r_{NCO}\right]^2 \tag{A10}$$

This is finally solved as an explicit quadratic expression:

$$(1-r_{NCO})^2\cdot\left(Z^{(-)}\right)^2+(2\cdot(1-r_{NCO})\cdot r_{NCO}-1)\cdot\left(Z^{(-)}\right)+{r_{NCO}}^2=0 \quad \text{(A11)}$$

This equation leads to a meaningful solution of $Z^{(-)}\in[0,1]$. The fraction of residual stress σ^*/σ_0 can be made equivalent to the fraction of permanent network strands, calculated from the remaining number of S-3 fragments, $(1-r_{NCO})^3$, and the probability that the 3 bonds have infinite continuation $\left(1-Z^{(-)}\right)^3$, with respect to the original number of network strands (initial number of S-3 fragments when $x=0$):

$$\sigma^*/\sigma_0=(1-r_{NCO})^3\cdot\left(1-Z^{(-)}\right)^3 \quad \text{(A12)}$$

Tetrafunctional thiol crosslinking agent

Following the same logics, it is be possible to define the extent of bond exchange for full stress relaxation and residual stress for materials crosslinked with a tetrafunctional thiol crosslinker. Taking 1 mol of tetrafunctional crosslinker as a reference, we define the concentration and capture probabilities of the tetrafunctional thiol species bearing (-) bonds, depending on the degree of bond exchange:

The distribution of diisocyanate an DG species bearing (+) bonds is somewhat changed, taking into consideration that a tetrafunctional thiol crosslinker is used (see Tables A.3 and A.4):

Following the same methodology, we define the expected weights $W^{(-)}$ and $W^{(+)}$:

$$W^{(-)}=P_{DG}^{(+)}\cdot\left(W^{(+)}+M_{DG}\right)+P_{I-2}^{(+)}\cdot\left(W^{(+)}+M_I\right)+P_{I-1}^{(+)}\cdot M_I$$

$$W^{(+)}=P_{S-4}^{(-)}\cdot\left(3\cdot W^{(-)}+M_S\right)+P_{S-3}^{(-)}\cdot\left(2\cdot W^{(-)}+M_S\right)+P_{S-2}^{(-)}\cdot\left(W^{(-)}+M_S\right)+P_{S-1}^{(-)}\cdot M_S \quad \text{(A13)}$$

The matrix coefficients are:

$$a_{-,+}=-P_{DG}^{(+)}-P_{I-2}^{(+)}=-\left(\frac{1-r_{NCO}+r_{NCO}\cdot(1-x)^2}{1-r_{NCO}\cdot x}\right)$$

$$a_{+,-}=-3\cdot P_{S-4}^{(-)}-2\cdot P_{S-3}^{(-)}-P_{S-2}^{(-)}$$

$$=-3\cdot(1-r_{NCO}\cdot x)^3-2\cdot3\cdot(1-r_{NCO}\cdot x)^2\cdot(r_{NCO}\cdot x)-3\cdot(1-r_{NCO}\cdot x)\cdot(r_{NCO}\cdot x)^2=$$

$$=-3\cdot(1-r_{NCO}\cdot x) \quad \text{(A14)}$$

Complete stress relaxation takes place at a given $x=x^*<1$. This occurs when the determinant of the matrix of coefficients is $1-a_{-,+}\cdot a_{+,-}=0$. It can be deduced that

$$x^*=1-\sqrt{1-\frac{2}{3\cdot r_{NCO}}} \quad \text{(A15)}$$

Full stress relaxation is only possible for $r_{NCO}\geq {r_{NCO}}^*$, with a threshold ${r_{NCO}}^*=2/3$ (determined for $x^*=1$)

For the calculation of the residual stress when $r_{NCO}<{r_{NCO}}^*$, we first calculate he extinction probabilities $Z^{(+)}$ and $Z^{(-)}$:

$$Z^{(-)}=P_{DG}^{(+)}\cdot Z^{(+)}+P_{I-2}^{(+)}\cdot Z^{(+)}+P_{I-1}^{(+)}$$

$$Z^{(+)}=P_{S-4}^{(-)}\cdot\left(Z^{(-)}\right)^3+P_{S-3}^{(-)}\cdot\left(Z^{(-)}\right)^2+P_{S-2}^{(-)}\cdot Z^{(-)}+P_{S-1}^{(-)} \quad \text{(A16)}$$

This transforms into the following expressions, by setting $x=1$:

$$Z^{(-)}=Z^{(+)}$$

$$Z^{(+)}=\left[(1-r_{NCO})\cdot Z^{(-)}+r_{NCO}\right]^3 \quad \text{(A17)}$$

The fraction of residual stress σ^*/σ_0 can be determined from the contribution of (a) S-4 fragments with 4 bonds with infinite continuation, (b) S-4 fragments with 3 bonds with infinite continuation and a finite continuation, (c) S-3 fragments with 3 bonds with infinite continuation, and (d) the initial number of S-4 fragments ($x=0$) with 4 bonds with infinite continuation. It must also be considered that the effective elastic contribution of the different crosslinks depending on the functionality is better modelled using a phantom network model [41]. The resulting expression for the residual stress is:

$$\sigma^*/\sigma_0=(1-r_{NCO})^4\cdot\left[\left(1-Z^{(-)}\right)^4+2\cdot\left(1-Z^{(-)}\right)^3\cdot Z^{(-)}\right]+(1-r_{NCO})^3\cdot(r_{NCO})\cdot\left[2\cdot\left(1-Z^{(-)}\right)^3\right] \quad \text{(A18)}$$

References

[1] J.-P.-P. Pascault, H. Sautereau, J. Verdu, R.J.J. Williams, Thermosetting polymers, Marcel Dekker, New York [etc.], 2002.

[2] I. Isarn, L. Bonnaud, L. Massagués, À. Serra, F. Ferrando, Enhancement of thermal conductivity in epoxy coatings through the combined addition of expanded graphite and boron nitride fillers, Prog. Org. Coatings. 133 (2019) 299–308, https://doi.org/10.1016/j.porgcoat.2019.04.064.

[3] W. Post, A. Susa, R. Blaauw, K. Molenveld, R.J.I. Knoop, A Review on the Potential and Limitations of Recyclable Thermosets for Structural Applications, Polym. Rev. 60 (2020) 359–388, https://doi.org/10.1080/15583724.2019.1673406.

[4] C.J. Kloxin, T.F. Scott, B.J. Adzima, C.N. Bowman, Covalent Adaptable Networks (CANs): A Unique Paradigm in Cross-Linked Polymers, Macromolecules 43 (2010) 2643–2653, https://doi.org/10.1021/ma902596s.

[5] D. Montarnal, M. Capelot, F. Tournilhac, L. Leibler, Silica-Like Malleable Materials from Permanent Organic Networks, Science (80-.). 334 (2011) 965–968. https://doi.org/10.1126/science.1212648.

[6] W. Alabiso, S. Schlögl, The Impact of Vitrimers on the Industry of the Future: Chemistry, Properties and Sustainable Forward-Looking Applications, Polymers (Basel). 12 (2020) 1660, https://doi.org/10.3390/polym12081660.

[7] W. Denissen, J.M. Winne, F.E. Du Prez, Vitrimers: permanent organic networks with glass-like fluidity, Chem. Sci. 7 (2015) 30–38, https://doi.org/10.1039/c5sc02223a.

[8] M. Capelot, D. Montarnal, F. Tournilhac, L. Leibler, Metal-Catalyzed Transesterification for Healing and Assembling of Thermosets, J. Am. Chem. Soc. 134 (2012) 7664–7667, https://doi.org/10.1021/ja302894k.
[9] F.I. Altuna, C.E. Hoppe, R.J.J. Williams, Epoxy vitrimers with a covalently bonded tertiary amine as catalyst of the transesterification reaction, Eur. Polym. J. 113 (2019) 297–304, https://doi.org/10.1016/j.eurpolymj.2019.01.045.
[10] L. Li, X. Chen, K. Jin, J.M. Torkelson, Vitrimers Designed Both To Strongly Suppress Creep and To Recover Original Cross-Link Density after Reprocessing: Quantitative Theory and Experiments, Macromolecules 51 (2018) 5537–5546, https://doi.org/10.1021/acs.macromol.8b00922.
[11] L. Li, X. Chen, J.M. Torkelson, Reprocessable Polymer Networks via Thiourethane Dynamic Chemistry: Recovery of Cross-link Density after Recycling and Proof-of-Principle Solvolysis Leading to Monomer Recovery, Macromolecules 52 (2019) 8207–8216, https://doi.org/10.1021/acs.macromol.9b01359.
[12] F. Gamardella, F. Guerrero, S. De la Flor, X. Ramis, À. Serra, A. Serra, A new class of vitrimers based on aliphatic poly(thiourethane) networks with shape memory and permanent shape reconfiguration, Eur. Polym. J. 122 (2019), 109361, https://doi.org/10.1016/j.eurpolymj.2019.109361.
[13] J. Shin, H. Matsushima, C.M. Comer, C.N. Bowman, C.E. Hoyle, Thiol−Isocyanate−Ene Ternary Networks by Sequential and Simultaneous Thiol Click Reactions, Chem. Mater. 22 (2010) 2616–2625, https://doi.org/10.1021/cm903856n.
[14] A. Ruiz De Luzuriaga, R. Martin, N. Markaide, A. Rekondo, G. Cabañero, J. Rodríguez, I. Odriozola, Epoxy resin with exchangeable disulfide crosslinks to obtain reprocessable, repairable and recyclable fiber-reinforced thermoset composites, Mater. Horizons. 3 (2016) 241–247, https://doi.org/10.1039/c6mh00029k.
[15] O. Konuray, S. Moradi, A. Roig, X. Fernández-Francos, X. Ramis, Thiol-Ene Networks with Tunable Dynamicity for Covalent Adaptation, ACS Appl. Polym. Mater. 5 (2023) 1651–1656, https://doi.org/10.1021/acsapm.2c02136.
[16] D.J. Fortman, R.L. Snyder, D.T. Sheppard, W.R. Dichtel, Rapidly Reprocessable Cross-Linked Polyhydroxyurethanes Based on Disulfide Exchange, ACS Macro Lett. 7 (2018) 1226–1231, https://doi.org/10.1021/acsmacrolett.8b00667.
[17] M. Pepels, I. Filot, B. Klumperman, H. Goossens, Self-healing systems based on disulfide–thiol exchange reactions, Polym. Chem. 4 (2013) 4955, https://doi.org/10.1039/c3py00087g.
[18] S.K. Schoustra, T. Groeneveld, M.M.J. Smulders, The effect of polarity on the molecular exchange dynamics in imine-based covalent adaptable networks, Polym. Chem. 12 (2021) 1635–1642, https://doi.org/10.1039/D0PY01555E.
[19] R.L. Snyder, C.A.L. Lidston, G.X. De Hoe, M.J.S. Parvulescu, M.A. Hillmyer, G. W. Coates, Mechanically robust and reprocessable imine exchange networks from modular polyester pre-polymers, Polym. Chem. 11 (2020) 5346–5355, https://doi.org/10.1039/C9PY01957J.
[20] R. Hajj, A. Duval, S. Dhers, L. Avérous, Network Design to Control Polyimine Vitrimer Properties: Physical Versus Chemical Approach, Macromolecules 53 (2020) 3796–3805, https://doi.org/10.1021/acs.macromol.0c00453.
[21] A. Roig, P. Hidalgo, X. Ramis, S. De la Flor, À. Serra, Vitrimeric Epoxy-Amine Polyimine Networks Based on a Renewable Vanillin Derivative, ACS Appl. Polym. Mater. 4 (2022) 9341–9350, https://doi.org/10.1021/acsapm.2c01604.
[22] O. Konuray, X. Fernández-Francos, X. Ramis, Structural Design of CANs with Fine-Tunable Relaxation Properties: A Theoretical Framework Based on Network Structure and Kinetics Modeling, Macromolecules (2023), https://doi.org/10.1021/acs.macromol.3c00482.
[23] X. Fernández-Francos, A.-O. Konuray, A. Belmonte, S. De la Flor, À. Serra, X. Ramis, Sequential curing of off-stoichiometric thiol-epoxy thermosets with custom-tailored structure, Polym. Chem. 7 (2016) 2280–2290, https://doi.org/10.1039/c6py00099a.
[24] X. Ramis, X. Fernández-Francos, S. De la Flor, F. Ferrando, A. Serra, Chapter 16 - Click-based dual-curing thermosets and their applications, in: Q. Guo (Ed.), Thermosets Struct. Prop. Appl. Second Ed., Elsevier, 2018: pp. 511–541. https://doi.org/10.1016/B978-0-08-101021-1.00016-2.
[25] D.P. Nair, N.B. Cramer, J.C. Gaipa, M.K. McBride, E.M. Matherly, R.R. McLeod, R. Shandas, C.N. Bowman, Two-Stage Reactive Polymer Network Forming Systems, Adv. Funct. Mater. 22 (2012) 1502–1510, https://doi.org/10.1002/adfm.201102742.
[26] A. Belmonte, X. Fernández-Francos, À. Serra, S. De la Flor, Phenomenological characterization of sequential dual-curing of off-stoichiometric thiol-epoxy systems: Towards applicability, Mater. Des. 113 (2017) 116–127, https://doi.org/10.1016/j.matdes.2016.10.009.
[27] F. Gamardella, V. Sabatini, X. Ramis, À. Serra, Tailor-made thermosets obtained by sequential dual-curing combining isocyanate-thiol and epoxy-thiol click reactions, Polymer (Guildf). 174 (2019) 200–209, https://doi.org/10.1016/j.polymer.2019.04.041.
[28] H. Matsushima, J. Shin, C.N. Bowman, C.E. Hoyle, Thiol-isocyanate-acrylate ternary networks by selective thiol-click chemistry, J. Polym. Sci. Part A Polym. Chem. 48 (2010) 3255–3264, https://doi.org/10.1002/pola.24102.
[29] C. Russo, À. Serra, X. Fernández-Francos, S. De la Flor, Characterization of sequential dual-curing of thiol-acrylate-epoxy systems with controlled thermal properties, Eur. Polym. J. 112 (2019) 376–388, https://doi.org/10.1016/j.eurpolymj.2018.12.048.
[30] A.O. Konuray, X. Fernández-Francos, X. Ramis, Curing kinetics and characterization of dual-curable thiol-acrylate-epoxy thermosets with latent reactivity, React. Funct. Polym. 122 (2018) 60–67, https://doi.org/10.1016/j.reactfunctpolym.2017.11.010.
[31] F. Gamardella, S. Muñoz, S. De la Flor, X. Ramis, A. Serra, Recyclable Organocatalyzed Poly(Thiourethane) Covalent Adaptable Networks, Polymers (Basel). 12 (2020) 2913, https://doi.org/10.3390/polym12122913.
[32] S. Huang, M. Podgórski, X. Han, C.N. Bowman, Chemical recycling of poly (thiourethane) thermosets enabled by dynamic thiourethane bonds, Polym. Chem. 11 (2020) 6879–6883, https://doi.org/10.1039/D0PY01050B.
[33] T. Isogai, M. Hayashi, Critical Effects of Branch Numbers at the Cross-Link Point on the Relaxation Behaviors of Transesterification Vitrimers, Macromolecules 55 (2022) 6661–6670, https://doi.org/10.1021/acs.macromol.2c00560.
[34] F.I. Altuna, C.E. Hoppe, R.J. Williams, Epoxy Vitrimers: The Effect of Transesterification Reactions on the Network Structure, Polymers (Basel). 10 (2018) 43, https://doi.org/10.3390/polym10010043.
[35] B. Zhang, Z.A. Digby, J.A. Flum, P. Chakma, J.M. Saul, J.L. Sparks, D. Konkolewicz, Dynamic Thiol-Michael Chemistry for Thermoresponsive Rehealable and Malleable Networks, Macromolecules 49 (2016) 6871–6878, https://doi.org/10.1021/acs.macromol.6b01061.
[36] B. Zhang, P. Chakma, M.P. Shulman, J. Ke, Z.A. Digby, D. Konkolewicz, Probing the mechanism of thermally driven thiol-Michael dynamic covalent chemistry, Org. Biomol. Chem. 16 (2018) 2725–2734, https://doi.org/10.1039/C8OB00397A.
[37] E.F. Gomez, S.V. Wanasinghe, A.E. Flynn, O.J. Dodo, J.L. Sparks, L.A. Baldwin, C. E. Tabor, M.F. Durstock, D. Konkolewicz, C.J. Thrasher, 3D-Printed Self-Healing Elastomers for Modular Soft Robotics, ACS Appl. Mater. Interfaces. 13 (2021) 28870–28877, https://doi.org/10.1021/acsami.1c06419.
[38] D.R. Miller, C.W. Macosko, A New Derivation of Post Gel Properties of Network Polymers, Macromolecules 9 (1976) 206–211, https://doi.org/10.1021/ma60050a004.
[39] D.R. Miller, E.M. Valles, C.W. Macosko, Calculation of Molecular Parameters for Stepwise Polyfunctional Polymerization, Polym. Eng. Sci. 19 (1979) 272–283.
[40] A.O. Konuray, X. Fernández-Francos, X. Ramis, Latent curing of epoxy-thiol thermosets, Polymer (Guildf). 116 (2017) 191–203, https://doi.org/10.1016/j.polymer.2017.03.064.
[41] A.J. Lesser, E. Crawford, The role of network architecture on the glass transition temperature of epoxy resins, J. Appl. Polym. Sci. 66 (1997) 387–395, https://doi.org/10.1002/(sici)1097-4628(19971010)66:2<387::aid-app19>3.0.co;2-v.
[42] D. Guzmán, X. Ramis, X. Fernández-Francos, À. Serra, New Catalysts For Diglycidyl Ether Of Bisphenol A Curing Based On Thiol-Epoxy Click Reaction, Eur. Polym. J. 59 (2014) 377–386, https://doi.org/10.1016/j.eurpolymj.2014.08.001.
[43] A.J. Melchor Bañales, M.B. Larsen, Thermal Guanidine Metathesis for Covalent Adaptable Networks, ACS Macro Lett. 9 (2020) 937–943, https://doi.org/10.1021/acsmacrolett.0c00352.